Supplementary Information

Wrapping silicon microparticles by using well-dispersed single-walled carbon nanotubes for the preparation of high-performance lithium-ion battery anode

Youngseul Cho[a], *Kyu Sang Lee*[b], *Shuqing Piao*[b], *Taek-Gyoung Kim*[c], *Seong-Kyun Kang*[c], *Sang Yoon Park*[d], *Kwanghyun Yoo*[*c], *Yuanzhe Piao*[*a,b,d]

[a] Program in Nano Science and Technology, Graduate School of Convergence Science and Technology, Seoul National University, 145 Gwanggyo-ro, Yeongtong-gu, Suwon-Si, Gyeonggi-do, 16229, Republic of Korea

[b] Department of Applied Bioengineering, Graduate School of Convergence Science and Technology, Seoul National University, 145 Gwanggyo-ro, Yeongtong-gu, Suwon-Si, Gyeonggi-do, 16229, Republic of Korea

[c] BETTERIAL Co., 307, 52, Sagimakgol-ro, Jungwon-gu, Seongnam-si, Gyeonggi-do, Republic of Korea

[d] Advanced Institutes of Convergence Technology, 145 Gwanggyo-ro, Yeongtong-gu, Suwon-si, Gyeonggi-do, 16229, Republic of Korea

*Corresponding authors

- E-mail:

*kyoo@betterial.io (K. Yoo)
*parkat9@snu.ac.kr (Y. Piao)

Fig. S1 Digital photographs for explaining freeze-drying of SiMP/CNT wrapping 9:1 composite.

Fig. S2 Digital photographs of (a) SWCNT dispersion, (b) SWCNT dispersion on a spatula, and (c) SWCNT coating on slide glass. Dispersion stability of the SWCNT dispersion. Digital photographs of SWCNT dispersion at (d) initial stage and (e) after 24 hours. Optical microscopy images of (f) SWCNT dispersion and (g) SWCNT powder. Each sample was prepared with a certain amount of water with sonication and then coated on the slide glass.

Fig. S3 SEM images of SiNP/CNT 9:1 composite with (a) low and (b) high magnification.

Fig. S4 SEM images of SiNP/CNT wrapping 8:2 composite with (a-c) low magnification and (d-e) high magnification.

Fig. S5 SEM images of SiMP/CNT wrapping 8:2 electrode with (a) low and (b and c) high magnification. SEM images of SiMP/CNT wrapping 9:1 electrode with (d) low and (e and f) high magnification.

Fig. S6 CV profiles of SiMP/CNT wrapping 8:2 electrode at a scan rate of 0.2 mV s^{-1} for 5 cycles.

Fig. S7 Galvanostat charge and discharge profiles of (a) 9:1 and (b) 8:2 electrodes at first steps of 0.2, 0.5, 1.0, 1.5, and 2.0 A g^{-1} of different C-rate sweep in rate performance.

Fig. S8 (a) Galvanostatic intermittent titration technique (GITT) measurement of SiMP/CNT wrapping 8:2 and 9:1 electrodes. (b) magnified view of the GITT profile. (c) Li^+ diffusion coefficient of SiMP/CNT wrapping 8:2 and 9:1 electrodes.

Fig. S9 HR-TEM images of (a) SiMP/CNT wrapping 8:2 and (b) SiMP/CNT wrapping 9:1 composites in cycled electrodes.

Equation S1 The equation for lithium-ion diffusion kinetics. Each component m_B, M_B, V_M, S, τ, $\triangle E_S$, and $\triangle E_\tau$ stand for active mass, molar mass, molar volume, the active surface area of the electrode, constant current time, voltage change, and total voltage change, respectively.

Table S1 Comparison chart of our work and reported Si/Carbon composite papers regarding preparation method, carbonaceous material with carbon content, and electrochemical performance.

Table S2 EIS parameters for the Fresh and 20 cycled symmetric cell of SiMP/CNT wrapping 9:1 and SiMP/CNT wrapping 8:2 electrodes.

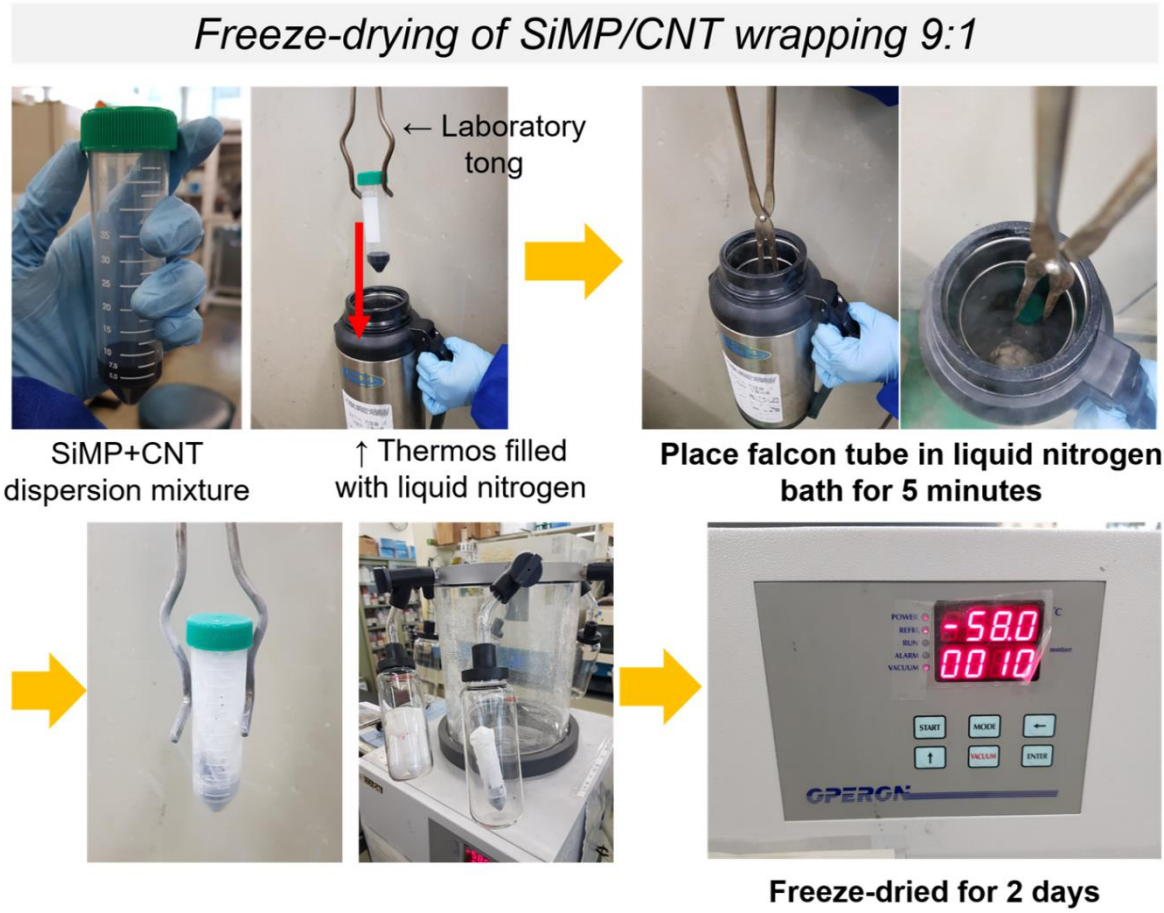

Fig. S1. Digital photographs for explaining freeze-drying of SiMP/CNT wrapping 9:1 composite.

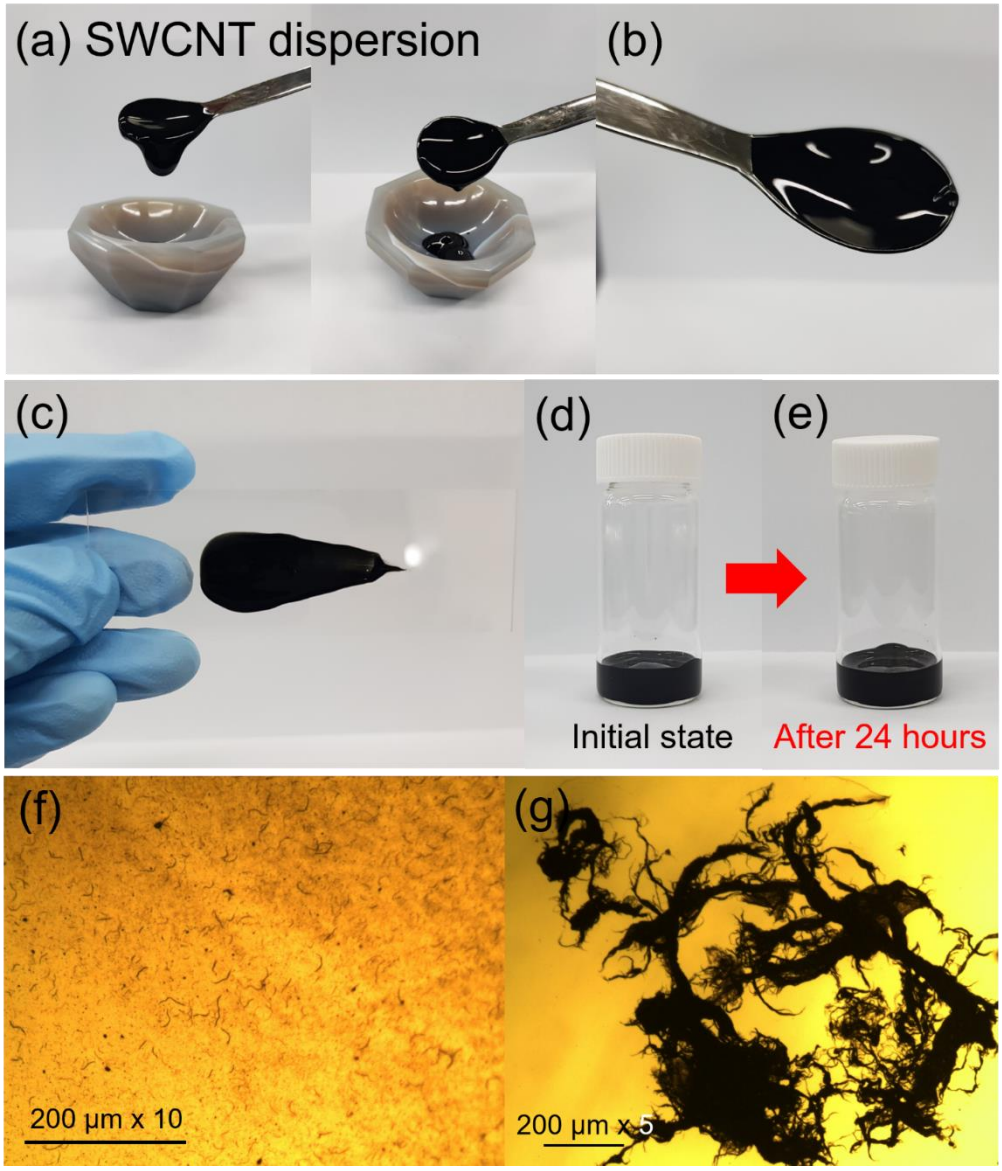

Fig. S2. Digital photographs of (a) SWCNT dispersion, (b) SWCNT dispersion on a spatula, and (c) SWCNT coating on slide glass. Dispersion stability of the SWCNT dispersion. Digital photographs of SWCNT dispersion at (d) initial stage and (e) after 24 hours. Optical microscopy images of (f) SWCNT dispersion and (g) SWCNT powder. Each sample was prepared with a certain amount of water with sonication and then coated on the slide glass.

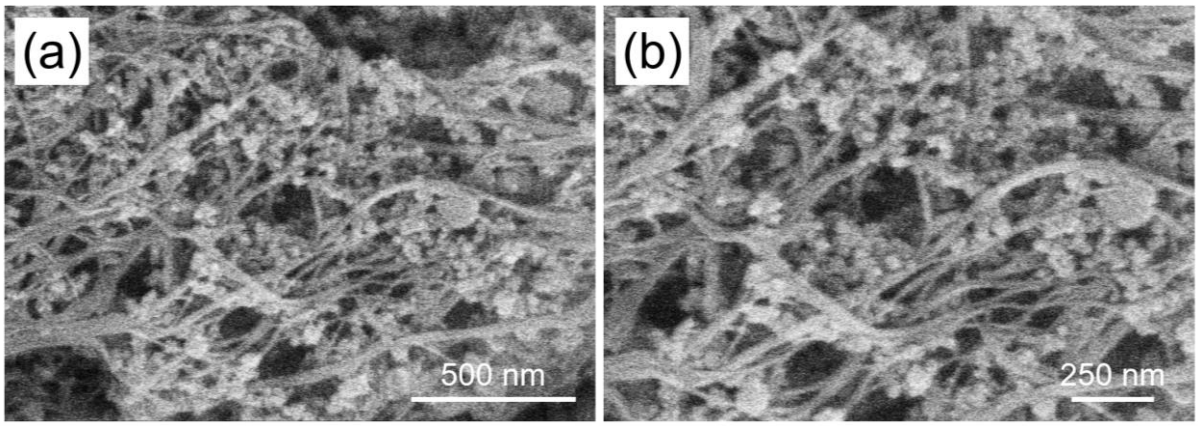

Fig. S3. SEM images of SiNP/CNT 9:1 composite with (a) low and (b) high magnification.

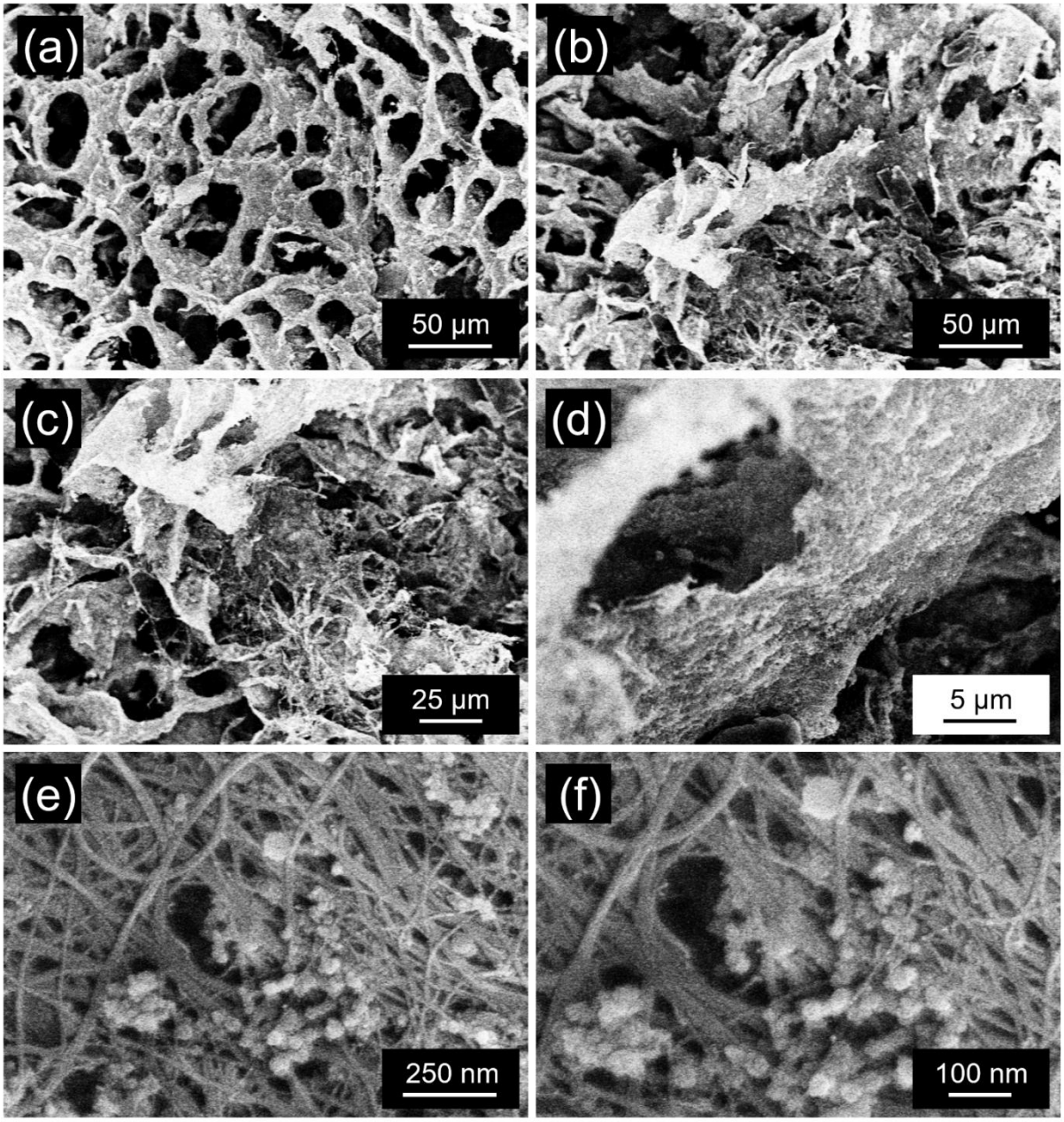

Fig. S4. SEM images of SiNP/CNT wrapping 8:2 composite with (a-c) low magnification and (d-e) high magnification.

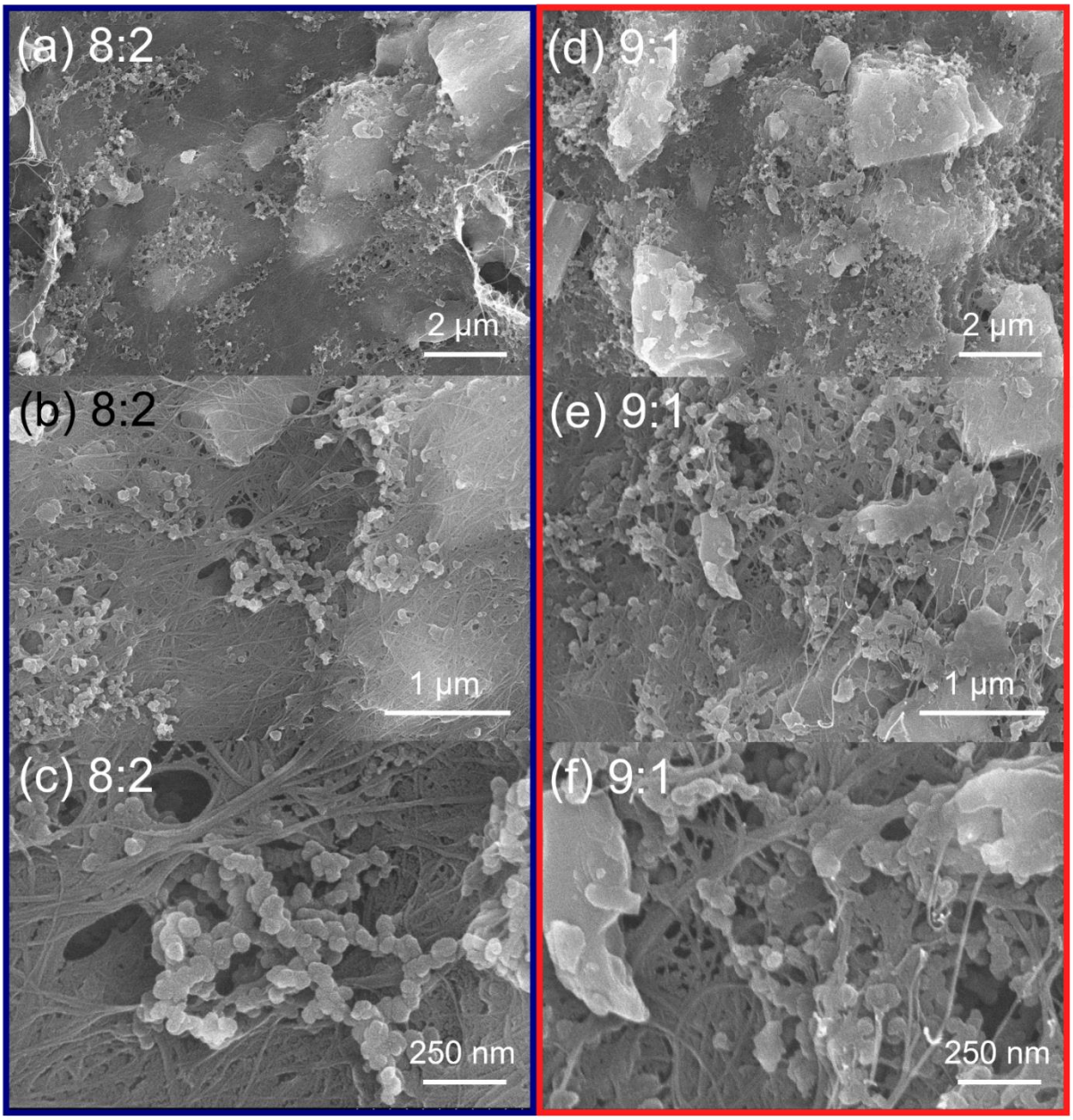

Fig. S5. SEM images of SiMP/CNT wrapping 8:2 electrode with (a) low and (b and c) high magnification. SEM images of SiMP/CNT wrapping 9:1 electrode with (d) low and (e and f) high magnification.

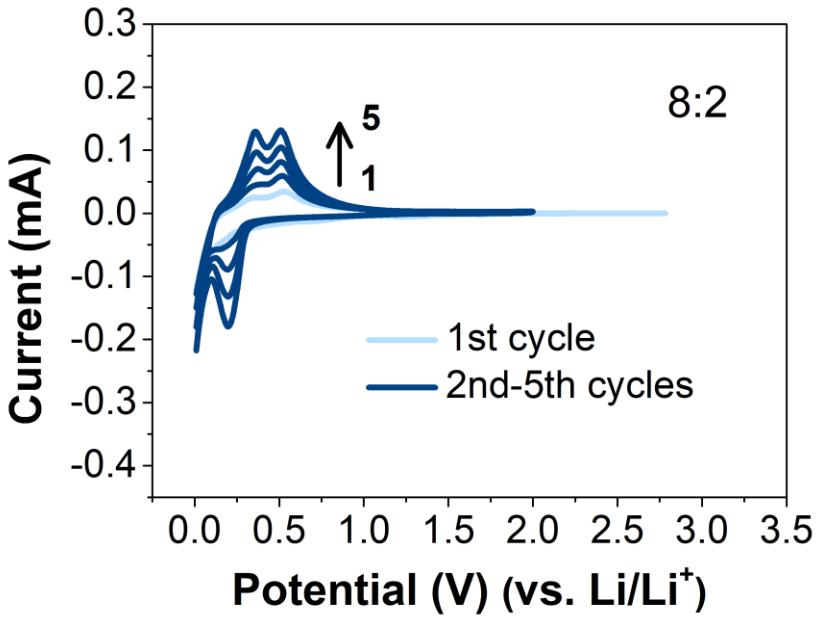

Fig. S6. CV profiles of SiMP/CNT wrapping 8:2 electrode at a scan rate of 0.2 mV s^{-1} for 5 cycles.

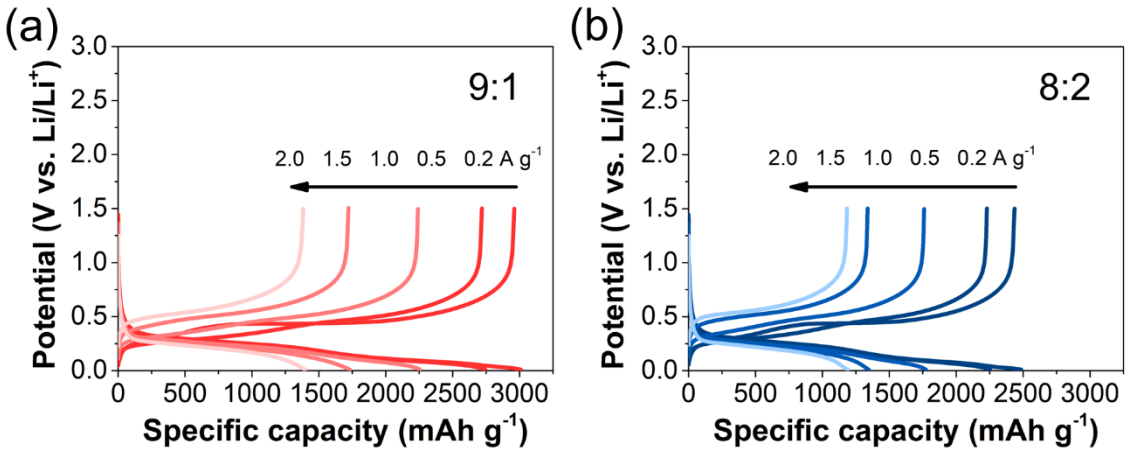

Fig. S7. Galvanostat charge and discharge profiles of (a) 9:1 and (b) 8:2 electrodes at first steps of 0.2, 0.5, 1.0, 1.5, and 2.0 A g^{-1} of different C-rate sweep in rate performance.

Equation S1. The equation for lithium-ion diffusion kinetics. Each component m_B, M_B, V_M, S, τ, $\triangle E_S$, and $\triangle E_\tau$ stand for active mass, molar mass, molar volume, the active surface area of the electrode, constant current time, voltage change, and total voltage change, respectively.

$$D_{Li} = \frac{4}{\pi\tau}\left(\frac{m_B V_M}{M_B S}\right)^2 + \left(\frac{\triangle E_S}{\triangle E_\tau}\right)^2$$

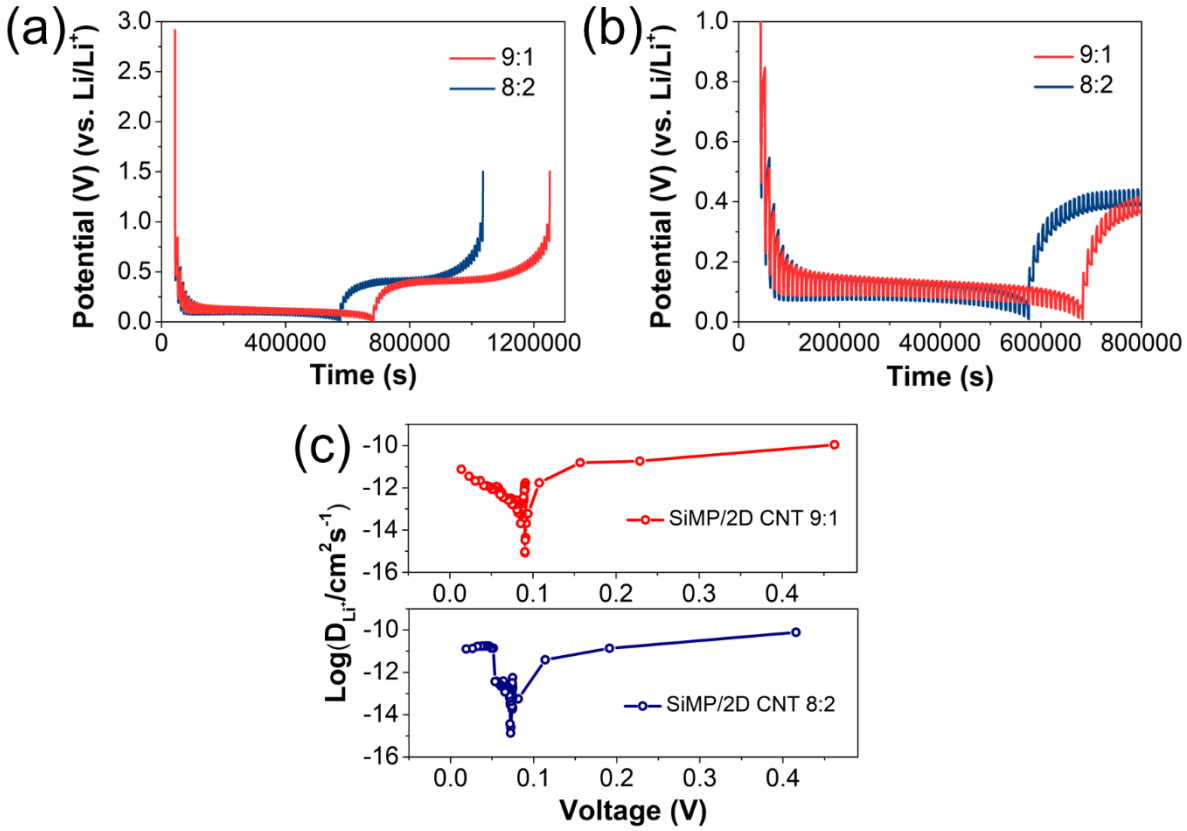

Fig. S8. (a) Galvanostatic intermittent titration technique (GITT) measurement of SiMP/CNT

wrapping 8:2 and 9:1 electrodes. (b) magnified view of the GITT profile. (c) Li^+ diffusion coefficient of SiMP/CNT wrapping 8:2 and 9:1 electrodes.

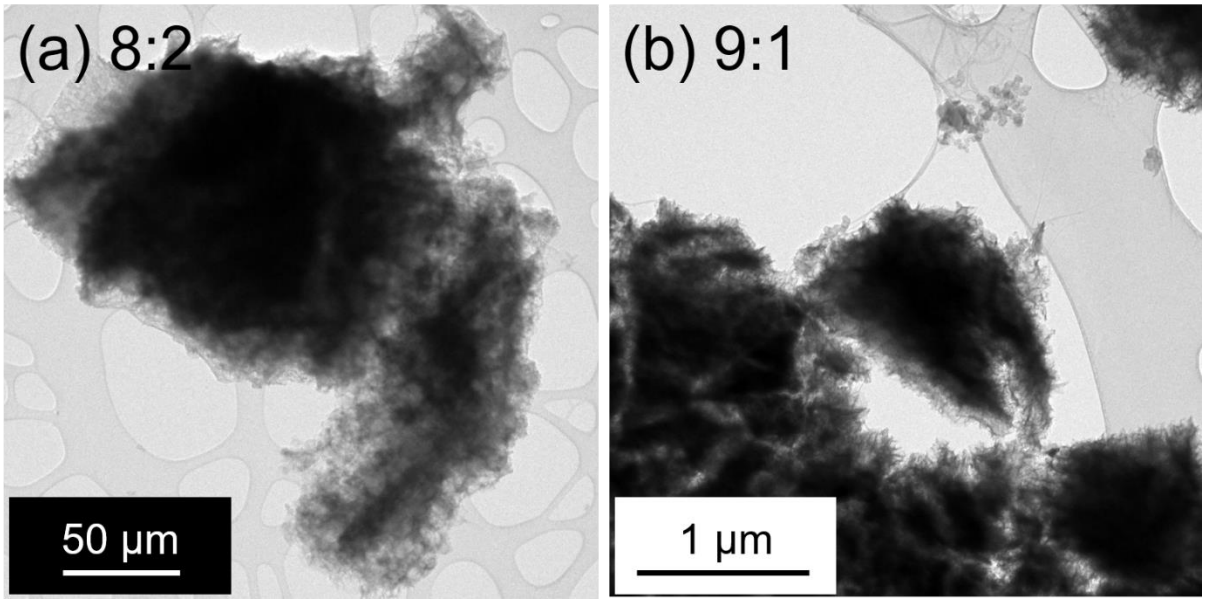

Fig. S9. HR-TEM images of (a) SiMP/CNT wrapping 8:2 and (b) SiMP/CNT wrapping 9:1 composites in cycled electrodes.

Table S1. Comparison chart of our work and reported Si/Carbon composite papers regarding preparation method, carbonaceous material with carbon content, and electrochemical performance.

	Synthetic method	**Silicon and carbonaceous material (C weight % in the composite)**	**Electrode preparation(active material:conductive additive:binder) (loading mass)**	**First specific capacity (mAh g^{-1})**	**Initial coulombic efficiency (%)**	**Cycle performance with capacity retention**	**Reference**
Silicon microparticle/2D CNT wrapping 9:1 composite (SiMP/CNT wrapping 9:1)	Freeze-drying	Silicon microparticle and Carbon nanotube dispersion (8.7%)	70:15:15 (0.7 mg/cm^2)	Charge and discharge capacity as 3160.7 and 3469.1 mAh g^{-1} at 0.1 A g^{-1}.	91.1%	85.87% (after 100 cycles at 1 A g^{-1})	**Our work**
3D Si-based gel	Gelation	Silicon microparticle and GO/CNT dispersion (34.35%)	70:15:15 (0.5~1.5 mg/cm^2)	Second charge and discharge capacity as 2892.81 and 3253.64 mAh g^{-1} at 420 mA g^{-1}	Second CE 88.91%	33.33% (reversible discharge capacity as 1085.3 mAh g^{-1} at 420 mAg^{-1} after 100 cycles)	[S1]
Nitrogen-doped graphitic carbon network on SiMPs (Si@pGN)	In-situ polymer pyrolysis and thermal graphitization by catalytic FeNPs	Silicon microparticle and Poly(vinyl pyrrolidone) (4.2%)	70:10:20 (0.7 mg/cm^2)	Reversible capacity as 3430 mAh g^{-1} at 0.05 C (1C = 3430 mA g^{-1})	90.6%	73.6% (after 100 cycles at 1C)	[S2]
Zinc-assisted Si/rGO nanocomposite (Si/rGO)	Zinc-assisted mechanochemical coating of reduced graphene oxide	Silicon microparticle and graphene oxide (24%)	80:10:10 (-mg/cm^2)	Initial discharge specific capacity as 1725 mAh g^{-1} at 0.1 A g^{-1}.	70.4%	67.9% (after 200 cycles at 0.2 A g^{-1})	[S3]
Graphene-encapsulated Silicon microparticle(SiMP@Gra)	Electroless eposition of Ni, graphene growth using Ni template, and acid etching	Silicon microparticle and graphene (9%)	90:0:10 (0.8 mg/cm^2 for cycle performance of half-cell data) The active material in binder solution stirred for 12	Initial reversible capacity as 3,300 mAh g^{-1} at 0.05C (1C = 4200 mAh g^{-1})	93.2%	85% (after 300 cycles at 0.5C)	[S4]

			hours				
Nanoporous silicon microparticles supported by CNTs composite (p-Si/CNT)	Low temperature molten salt process	Nanoporous silicon microparticles and CNT (55.17%)	70:20:10 (0.8-1.2 mg/cm^2)	Initial charge and discharge capacity as 973 and 1841.4 mAh g-1 at 0.1 A g^{-1}	52.8%	78% (after 100 cycles at 0.5 A g^{-1})	[S5]
Graphene cage-encapsulated Si skin-sealed mesoporous Si microparticle composite (Mp-Si@Si@G)	Electroless deposition of Ni catalyst and CVD growth of graphene	Mesoporous Si microparticle and graphene (8%)	90:0:10 (0.68 mg/cm^2) The active material in the binder solution stirred for 12 hours	Initial delithiation and lithiation capacity as 2834 and 3197 mAh g^{-1} at 0.05C (1C = 4200 mA g^{-1})	88.7%	Specific capacity as 1246 mAh g^{-1} after 300 cycles at 0.5C	[S6]
Interconnected porous silicon/carbon composite (Si/C+C-900-HF)	Rochow reaction using CH_3Cl gas over Cu-based catalyst under the mild reaction	Porous silicon and carbon (35.9%)	80:10:10 (2.0-3.0 mg/cm^2)	First charge and discharge capacity as 856.5 and 1241.7 mAh g^{-1} at 50 mA g^{-1}	69.0%	Discharge capacity as 732.1 mAh g^{-1} after 100 cycles at 50 mA g^{-1}	[S7]
Silicon-graphite-carbon composite with the alkaline solution for 15 minutes (Si-G-C-15)	Ball milling and NaOH treatment	Silicon microparticle, graphite, and polyacrylonitrile-derived carbon (60%)	60:20:20 (0.98 mg/cm^2)	The specific discharge capacity at the second cycle is 1353 mAh g^{-1} at 0.2 A g^{-1}	-	71.34% (After 100 cycles at 0.2 A g^{-1})	[S8]
Reduced graphene oxide-sheltered overlapped graphene-coated silicon microparticles composite (mSi@OG@RGO)	Gel formation and carbonization	Silicon microparticle and graphene (22%)	80:10:10 (1.0-1.5 mg/cm^2)	-	78%	Average capacity above 1750 mAh g^{-1} over more than 150 cycles at 2 A g^{-1}	[S9]
Silicon@Germanium@Carbon composite (Core@shell) (Si@Ge@C)	Thermal decomposition	Submicron silicon particle and carbon (-%)	80:8:12 (0.5-0.7 mg/cm^2)	-	82%	80% (200 cycles at 2A g^{-1})	[S10]
Silicon/CNTs synthesized via CVD at 950˚C for 2	CVD method	Silicon microparticle and CNT (66.28%)	70:10:20 (-mg/cm^2)	The first charge and discharge capacity as 1826.5 and 2266.5 mAh g^{-1}	80.59%	656.6 mAh g^{-1} after 100 cycles at 0.1 A g^{-1}	[S11]

hours composite (Si/CNTs950-2)				at 0.1 A g^{-1}.			
Vertical graphene on porous microsilicon /nanosilver hybrid composite (VG-PMSi@Ag)	Thermal chemical vapor deposition	Silicon microparticle and graphene (-%)	60:20:10 (0.53-1.63 mg/cm^2)	The initial discharge capacity as 3121.6 mAh g^{-1} at 0.1 A g^{-1}.	-	1045.2 mAh g^{-1} after 300 cycles at 1 A g^{-1}	[S12]

Table S2. EIS parameters for the Fresh and 20 cycled symmetric cell of SiMP/CNT wrapping 9:1 and SiMP/CNT wrapping 8:2 electrodes.

Fresh symmetric cell (before cycling)				
Sample	**R_s (Ω)**	**R_{SEI} (Ω)**	**R_{ct} (Ω)**	**Reduced Chi-square**
SiMP/CNT wrapping 9:1	3.40 ± 0.13	-	3.01 ± 0.13	6.38×10^{-4}
SiMP/CNT wrapping 8:2	4.91 ± 0.04	-	3.31 ± 0.04	8.19×10^{-7}
20 cycled symmetric cell				
Sample	**R_s (Ω)**	**R_{SEI} (Ω)**	**R_{ct} (Ω)**	**Reduced Chi-square**
SiMP/CNT wrapping 9:1	2.69 ± 0.38	7.50 ± 4.57	22.67 ± 7.71	2.35×10^{-5}
SiMP/CNT wrapping 8:2	5.01 ± 0.16	14.45 ± 3.75	29.83 ± 14.05	2.25×10^{-5}

References

[S1] F. C. Lyu, Z. F. Sun, B. Nan, S. C. Yu, L. J. Cao, M. Y. Yang, M. C. Li, W. X. Wang, S. F. Wu, S. S. Zeng, H. T. Liu and Z. G. Lu, ACS Appl. Mater. Interfaces, 2017, 9, 10699-10707.

[S2] G. Song, M. J. Kwak, C. Hwang, C. An, S. Kim, S. Lee, S. Choi, H. K. Song, J. H. Jang and S. Park, ACS Appl. Energy Mater., 2021, 4, 10050-10058.

[S3] Z. Q. Zhao, X. Cai, X. Y. Yu, H. Q. Wang, Q. Y. Li and Y. P. Fang, Sustain. Energ. Fuels, 2019, 3, 1258-1268.

[S4] Y. Z. Li, K. Yan, H. W. Lee, Z. D. Lu, N. Liu and Y. Cui, Nat. Energy, 2016, 1.

[S5] Q. L. Zhang, B. J. Xi, W. H. Chen, J. K. Feng, Y. T. Qian and S. L. Xiong, Nano Res., 2022, 15, 6184-6191.

[S6] J. Y. Wang, L. Liao, H. R. Lee, F. F. Shi, W. Huang, J. Zhao, A. Pei, J. Tang, X. L. Zheng, W. Chen and Y. Cui, Nano Energy, 2019, 61, 404-410.

[S7] Z. L. Zhang, Y. H. Wang, W. F. Ren, Q. Q. Tan, Y. F. Chen, H. Li, Z. Y. Zhong and F. B. Su, Angew. Chem. –Int. Edit., 2014, 53, 5165-5169.

[S8] F. F. Zhao, M. Zhao, Y. R. Dong, L. Ma, Y. Zhang, S. L. Niu and L. M. Wei, Powder Technol., 2022, 404.

[S9] X. H. Zhang, R. Y. Guo, X. L. Li and L. J. Zhi, Small, 2018, 14.

[S10] K. Mishra, K. George and X. D. Zhou, Carbon, 2018, 138, 419-426.

[S11] P. Guan, W. Zhang, C. Y. Li, N. Han, X. C. Wang, Q. F. Li, G. J. Song, Z. Peng, J. J. Li, L. Zhang and X. Y. Zhu, J. Colloid Interface Sci., 2020, 575, 150-157.

[S12] Y. C. Mo, S. C. Li and J. Yu, ACS Appl. Nano Mater., 2022, 5.